INJ INTERNATIONAL NEUROUROLOGY JOURNAL

# DFS: Distributed Fusion Segmentation for Kidney Tumor using CT scan and Clinical Data Modalities

**Saurra Kavitha, Bukittla Sandhya, Mr. P .Kiran Rao, Talari Nagamani, Kadiyala Chandika**
Department of Computer Science and Engineering (Artificial Intelligence) Ravindra College Of Engineering For Women,Kurnool,AP,India.
Department of Computer Science and Engineering (Artificial Intelligence) Ravindra College Of Engineering For Women,Kurnool,AP,India.
Sr Asst Professor Department of Computer Science and Engineering, Ravindra College of Engineering for Women, Kurnool, AP, India.
Department of Computer Science and Engineering Ravindra College Of Engineering For Women,Kurnool,AP,India.
Department of Computer Science and Engineering Ravindra College Of Engineering For Women,Kurnool,AP,india.

## Abstract

Kidney tumors are a prevalent form of cancer that affects 75,000 individuals annually. Segmentation of kidney tumors is a critical step in accurate diagnosis, treatment planning, and evaluation of treatment outcomes. However, due to the complexity of the kidney structure and the variability of tumor shapes and sizes, segmentation remains a challenging task.

(1) Background:

With traditional machine learning algorithms require feature engineering, deep learning techniques such as CNNs can automatically learn features from the CT scan. However, training these models 6requires a large number of parameters, which can be time-consuming, and the inference time can also

be high. Furthermore, CNN-based methods may struggle with small and irregularly shaped .

(2) Method: Our approach, called DFS (Distributed Fusion Segmentation), combines both CT scan and clinical data modalities in a distributed fusion model. The DFS model consists of two main modules: the CT-based segmentation module and the clinical data-based segmentation module.

The CT-based module uses a deep convolutional neural network (CNN) to segment kidney tumor regions from CT scans, while the clinical data- based module uses various clinical data modalities, including patient age, gender, tumor location, and histology, to classify the kidney risk during its progression. The two modules then undergo a distributed fusion process that combines the segmented regions from both modules to produce a final segmentation mask.

(3) Results: The DFS model was trained and tested on a large dataset of CT scans and clinical data from kidney tumor patients, and it achieved state-of-the-art performance in tumor segmentation.

(4) Conclusion: Our results demonstrate that the integration of clinical data modalities into the segmentation process can significantly improve segmentation accuracy and reduce false positives. Moreover, the DFS model's distributed fusion approach allows for a more comprehensive and accurate segmentation of kidney tumours, which can lead to improved diagnosis, 22treatment planning, and evaluation of treatment outcomes.

**KEYWORDS:** Distributed Data Parallel; Kidney Tumour; Light Weight segmentation; GRU; Dense, Depth wise Separable, Stocastic Gradiant Descent, Distributed Fusion segmentation; CT scan ; clinical records;).

## Introduction

The kidneys play a crucial role in the body's fluid and solute balance, hormone secretion, and blood pressure regulation [1][2]. However, kidney diseases and cancer are significant health issues, with a lifetime risk of around 1 in 75 individuals. Renal carcinoma is a urinary illness that affects more than 400,000 people annually and is responsible for about 175,000 deaths.

RCC is the third most prevalent type of cancer, and the incidence rate has grown by 2 percentage annually during the last two decades. The majority of kidney tumours [2] are malignant, with clear cell renal cell carcinoma [3] accounting for 80-90 Percentage of all kidney malignancies. Although the aetiology of kidney cancer [4] remains unknown, several risk factors have been identified. Currently, radical and partial nephrectomy are the only available treatments for kidney tumours. Early detection of kidney tumours [5] is difficult as they can grow for a lengthy period of time without manifesting any symptoms.



ISSN:2093-4777 | E-ISSN:2093-6931
**DOI**: 10.5123/inj.2024.1.inj46
Vol. 28 Iss. 1 (2024)

Detection of more than half of renal cell carcinoma patients may be due to coincidence. Numerous techniques are utilized in clinical procedures for the diagnosis and prognosis of kidney disease. Medical professionals employ tests to assess kidney risk factors [6] such as blood pressure, blood, urine, white blood cells, and smoking history. Imaging techniques such as CT scans, MRI, or PET scans enable physicians to detect kidney tumors or other abnormalities. In some cases, a biopsy may be recommended to obtain a sample of cells from a suspicious area of the kidneys. As shown in Fig. 1 tumor and internal structure of kidney organ is a complex structure.

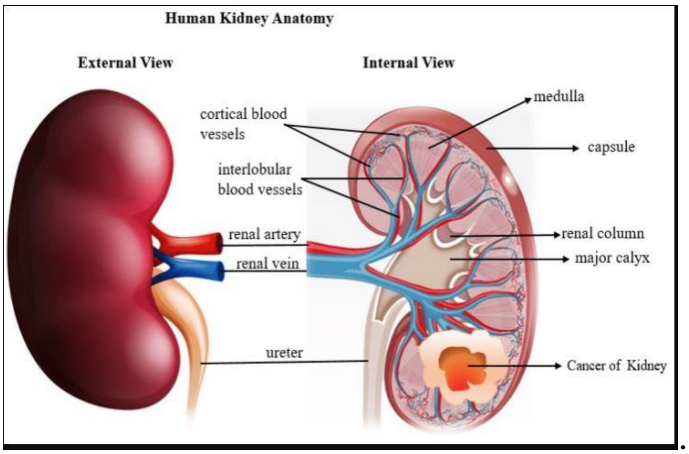


**Figure 1. Human kidney anato**

To assist experts medical imaging has become a valuable tool in detecting and di- agnosing various diseases, including cancer. Computed tomography (CT) [7] scans are commonly used to visualize internal organs and tissues, including the kidneys. However, accurately identifying and segmenting tumors in CT images [7] can be challenging, as tumors can have irregular shapes and sizes. Automated segmentation techniques using deep learning have shown promising results in accurately identifying and delineating tumors in medical images. In particular, convolutional neural networks (CNNs) [8] have demonstrated excellent performance in image segmentation tasks. In this context, the aim of this study is to develop a novel approach for kidney tumor segmentation in CT images[7] using deep learning techniques. Our approach will leverage the power of CNNs[8] to accurately segment kidney tumors[7][8], which will have important implications for cancer diagnosis and treatment. In addition, the clinical data records [9] of Kidney disease patients can provide important information on their health history, including previous diagnoses, medications, laboratory results, and imaging studies [9]. These records can be used to identify risk factors for kidney tumors, such as hypertension, diabetes, and smoking, which can guide screening and monitoring efforts. Furthermore, the progression of KD can also provide insight into the prognosis of kidney tumors. As KD advances, it can cause structural changes in the kidneys, such as cysts or scarring, which can mimic the appearance of tumors on imaging studies [10][11].

Therefore, understanding the extent and severity of KR can help prognosis of tumor and guide treatment decisions. To address kidney risk and tumor progression, a comprehensive approach that combines CT scan imaging [13] and clinical data [12] is essential. Kidney risk (KR) is often asymptomatic, and the diagnosis is made through blood and/or urine testing. Early identification and increased awareness of KR are crucial, and a person with KR risk factors should undergo routine evaluation. To accurately predict kidney disease using the fewest possible indicators, machine learning models such as deep neural networks can be used to analyze clinical data records. Similarly, for tumor segmentation, a distributed data parallel lightweight model can be used to effec tively segment the tumor from the CT scan images. This can aid in accurate diagnosis and prognosis of kidney tumors, leading to better treatment outcomes.

By Combining CT Scan imaging and clinical data, clinicians can develop a comprehensive understanding of the patient's condition, which can inform treatment decisions and improve patient outcomes.The reminder of this paper is organized as follows section 2 presents the related work to detect CT images and clinical records. Section 3 describes the materials and methods applied to fuse CT scan image dataset and clinical dataset using lightweight distributed data parallel algorithm. Section 4 shows the experiments and results. Lastly section 5 presents the discussion and conclusions

## Related Works

This section provides a review of relevant literature on the use of machine learning and deep learning techniques for the early detection and classification of Kidney tumor and Kidney Risk ( KR) complications based on CT scans and clinical data modalities. The studies reviewed employed various methods, including support vector machines, random forests, convolutional neural networks, and recurrent neural networks, to identify early signs of complications. Clinical data and CT scan images are valuable sources of information in medical diagnosis, treatment planning, and research for Kidney disease. CT scans are widely used in clinical practice for the detection and characterization of various diseases, including cancer, cardiovascular diseases, and neurological disorders. However, the interpretation of CT scan images can be challenging due to the complexity of anatomical structures and variations in image quality. Accurate and efficient analysis of CT scans requires advanced computational methods, such as image processing and machine learning.

**2.1. Clinical Data Modality :** The following studies provides a review of various studies in the field of machine learning applied to the prediction of Kidney Disease (KD). A significant number of research studies have been conducted using different machine learning algorithms to build models that aid in the prediction of various diseases and health-related issues. In the area of KD prediction, researchers have employed different techniques, including Deep Neural Network (DNN)[14], Artificial Neural Network (ANN)[15], Logistic Regression (LR)[16], Random Forest (RF)[17], Naïve Bayes (NB)[18], and Decision Tree (DT)[19]. Several studies have used various machine learning techniques, such as DNN, ANFIS, and neuro-fuzzy algorithms[20], to predict and diagnose different medical conditions. For example, Ge et al. (2019) achieved high accuracy in predicting Parkinson's disease[21] severity using DNN and biomedical voice measurements. Ayon and Islam (2019)[22] proposed a strategy for diagnosing diabetes with a high accuracy rate using DNN and the PIM Indian Diabetes dataset. Shafi et al. (2020) [23] developed a machine learning-based solution to kidney risk with renal disease using eGFRMORD using DNN and achieved a high accuracy rate with the MLP algorithm. Other studies focused on predicting chronic kidney disease (CKD) using various machine learning models, such as ANN, neuro-fuzzy algorithms, and DNN, with accuracy rates ranging from 84.41 Per to 100 Percentage. Overall, these studies demonstrate the potential of machine learning in diagnosing and predicting medical conditions. In summary, numerous studies have been conducted on KD prediction using various AI techniques, including DNN, ANN, LR, RF, NB, and DT. Although DNN models have been used less frequently than other techniques in KD prediction, they have shown promise in achieving better results.

**2.2. Related Works on CT scan image for Kidney tumor segmentation:**

Semantic segmentation involves identifying and labeling regions in 3D imaging such as CT or MRI scans. This technique has various applications such as radiation therapy targeting, patient-specific surgical simulations, and disease diagnosis and prognosis. How- ever, clinical translation of these applications depends on automating the segmentation process.

This has led to the rise of automatic semantic segmentation of biomedical imaging as a crucial research area. Despite unique challenges posed by the third dimension, recent studies have demonstrated impressive performance on the 3D segmentation of anatomical structures and lesions in cross-sectional imaging using deep learning methods. Deep neural networks (DNNs) dominate the design space for any given task, including 3D segmentation, and researchers are continually exploring this space for optimal performance. However, the high computational cost of training DNNs means that most studies proposing new DNN architectures lack comprehensive benchmarking against the state-of-the-art.

U-Net [24] and its 3D variants are some of the earliest proposed methods for DL-based medical image segmentation, and numerous modifications have been proposed since then. Isensee et al [26]. recently demonstrated state-of-the-art performance using only a U-Net [24] and a novel methodology to search a small space of hyperparameters and preprocessing procedures, termed nnU-Net[25]. Despite attempts to enhance it, nnU-Net demonstrated top performance in the recent KiTS19 challenge[27], one of the first grand challenges on 3D segmentation held after nnU-Net[25] demonstrated its dominant performance and implementation was released.

## Materials and Methods:

In this section three different models will be presented, a predictive model using the clinical dataset [? ] to identify the kidney risk factors, a segmentation model using the CT scan images to segment kidney tumors. Then finally, a novel algorithm called Distributed fusion segmentation will be presented.

3.1. Kidney Risk Classification Using GRU Model

### 3.1.1. Data preprocessing

The Deep learning and machine learning models require high-quality data to perform well, which is why the KD dataset [? ] must be pre-processed before use. This dataset contains 24 columns and 400 rows, with a binary output column indicating whether a patient has kidney disease (KD) or not. The KD dataset is incomplete in some respects, with certain variables missing values that must be completed using various techniques such as transforming continuous qualities into discrete features.

During pre-processing, categorical values must be encoded into numerical values since most deep learning and machine learn- ing models only accept numerical input. One approach to achieve this is through categorical embedding [? ], where each category is represented as a vector of floating-point values. In the KD dataset, the variables ['age','bp','al','su','bgr','bu','sc','sod','pot','hemo'] are nu- merical and its statistical analysis is described in Table 1, while['rbc','sg','pc','pcc','ba','pcv','wc','rc','htn','dm','cad','appet','pe','ane'] are categorical data values like yes / no.

Fig. 2 provides a breakdown of the variables in the KD dataset. It is important to note that the KD dataset has certain limitations, such as the presence of erroneous reports and the possibility of missing values. These issues addressed during pre-processing to ensure that the dataset is appropriate for use in deep learning and machine learning models.

| | count | mean | std | min | 25 % | 50% | 75% | max |
|---|---|---|---|---|---|---|---|---|
| id | 400 | 199.5 | 115.6143 | 0 | 99.75 | 199.5 | 299.25 | 399 |
| age | 391 | 51.48338 | 17.16971 | 2 | 42 | 55 | 64.5 | 90 |
| bp | 38 | 76.46907 | 13.68364 | 50 | 70 | 80 | 80 | 180 |
| sg | 353 | 1.017408 | 0.005717 | 1.005 | 1.01 | 1.02 | 1.02 | 1.025 |
| al | 354 | 1.016949 | 1.352679 | 0 | 0 | 0 | 2 | 5 |
| su | 351 | 0.450142 | 1.099191 | 0 | 0 | 0 | 0 | 5 |
| bgr | 356 | 148.0365 | 79.28171 | 22 | 99 | 121 | 163 | 490 |
| bu | 381 | 57.42572 | 50.50301 | 1.5 | 27 | 42 | 66 | 391 |
| sc | 383 | 3.072454 | 5.741126 | 0.4 | 0.9 | 1.3 | 2.8 | 76 |
| sod | 313 | 137.5288 | 10.40875 | 4.5 | 135 | 138 | 142 | 163 |
| pot | 312 | 4.627244 | 3.193904 | 2.5 | 3.8 | 4.4 | 4.9 | 47 |
| hemo | 348 | 12.52644 | 2.912587 | 3.1 | 10.3 | 12.65 | 15 | 17.8 |

**Table 1. Statistical Analysis of Numerical Values**

INJ INTERNATIONAL NEUROUROLOGY JOURNAL

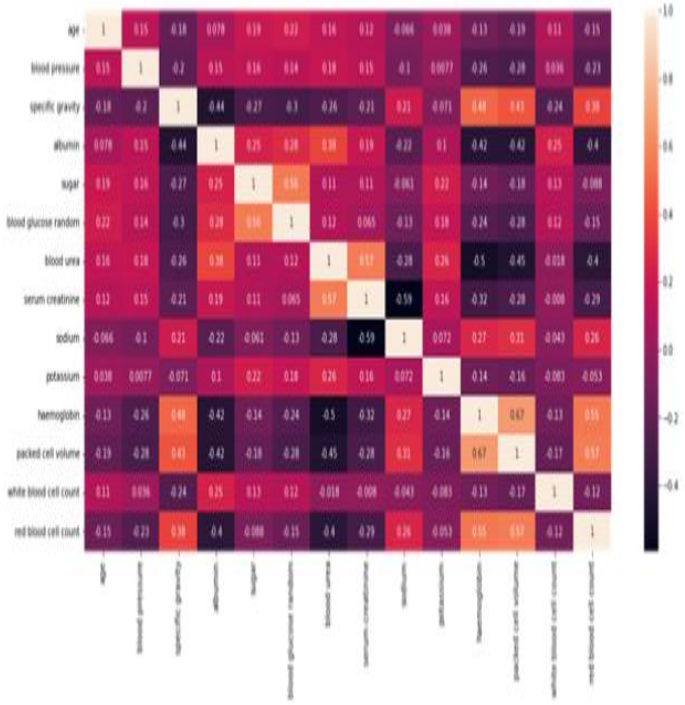


**Figure 2. Human kidney anatomy3.1.2. Kidney Risk Classification using clinical records**

To classify the kidney risk a custom deep learning model is proposed with Gated Recurrent layer units (GRU)[30]. The GRU[30] model for the KD dataset consists of multiple layers designed to process a sequence of input features and produce a binary classification output. The first layer is an input layer that takes in a sequence of features, where each feature has a dimension of 1.

The input sequence has a shape of (sequencelength, numfeatures), where sequencelength is the length of the input sequence and numfeatures is the number of input features i.e. 25 features. The next layer is a GRU layer that takes in the input sequence and processes it using a set of GRU units. The output of the GRU layer has a shape of (sequencelength, numgru-units), where numgru-units is the number of GRU units.

The GRU layer has learnable parameters that are trained during the model training process. The output of the GRU layer [30] is then fed into one or more fully connected layers, also known as dense layers. The fully connected layer(s) can have a varying number of neurons, which are also learnable parameters trained during the model training process. The output of the fully connected layer(s) has a shape of (numneurons,), where numneurons is the number of neurons in the fully connected layer(s).

Finally, the output of the fully connected layer(s) is fed into an output layer that produces the final output. In the case of the KD dataset, which is a binary classification problem, the output layer consists of a single output neuron with a sigmoid activation function that produces a probability distribution over the two possible classes (normal or abnormal).

The output layer has learnable parameters that are trained during the model training process.

The GRU unit is represented as follows: Let xt be the input feature vector at time t, ht be the hidden state vector at time t, and yt be the output vector at time t. The GRU layer [30] unit has the listed gates as represented in equations (1) (2) (3) (4) and layer unit shown in Fig 3.



ISSN:2093-4777 | E-ISSN:2093-6931
**DOI**: 10.5123/inj.2024.1.inj46
Vol. 28 Iss. 1 (2024)

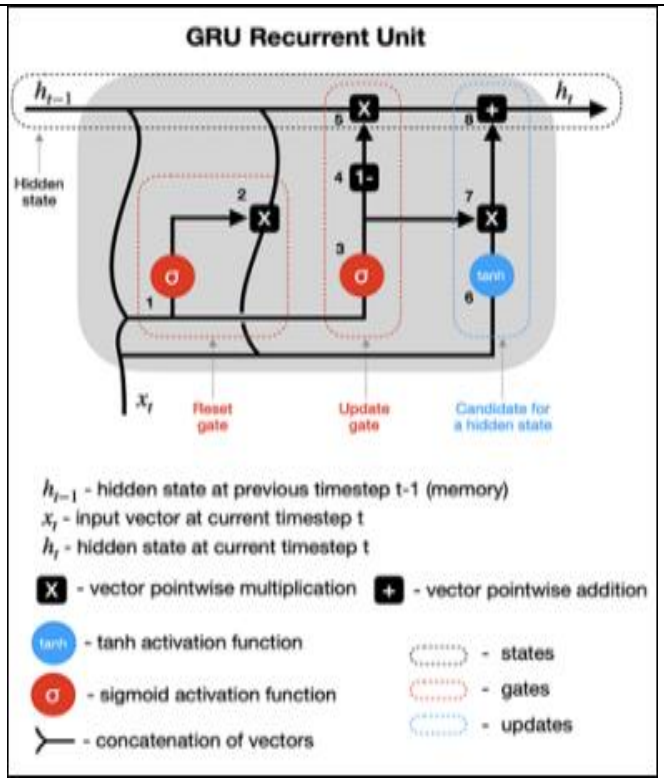


**Figure 3. Human kidney anatomy**

Where is the sigmoid function, represents matrix multiplication W, U, Wr, Ur, Wz, Uz, b, br, bz are the learnable parameters of the model. In this model, the input sequence is a sequence of vectors, where each vector has a dimension of 25 (the number of features). The GRU layer takes in this sequence of vectors and processes it using a set of GRU units [30]. The output of the GRU layer is a sequence of hidden state vectors, where each hidden state vector has a dimension of numgruunits.A f tertheGRUlayer[30], the output sequenceis of edintoa fully conatenation of vector.

### 3.2. RUSP-Net for Kidney Tumor Segmentation

#### 3.2.1. Data Preprocessing

The KiTs challenge dataset [27] is a commonly utilized dataset for evaluating kidney tumor segmentation techniques. It includes high contrast CT scans of patientswho underwent partial or radical nephrectomy for one or more kidney tumors at the University of Minnesota Medical Center between 2010 and 2018 [27]. The dataset comprises scans with varying resolutions from 0.437 to 1.04 mm in plane resolution and slice thickness ranging from 0.5 mm to 5.0 mm.

The dataset comes with ground-truth masks for healthy kidney tissue and tumors for each case as shown in Fig 4, manually generated by medical students under experienced radiologists' guidance, using only CT scan image axial projections. The dataset is provided in the standard NIFTI format [27]with shape (num slices, height, width) and has been utilized as a benchmark for various kidney tumor segmentation methods, including proposed model, which was assessed on this dataset. The use of this dataset is advantageous as it provides a diverse set of CT scans with varying resolutions and slice thicknesses, allowing for the evaluation of the robustness and generalization of segmentation techniques. Furthermore, the ground-truth masks were generated under expert guidance, ensuring the accuracy and reliability of the annotations.

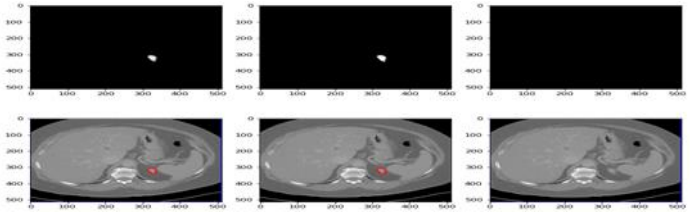

**Figure 4. An example of CT scan images from the KiTs19 Challenge which gives abdominal andground truth images [27] dataset**

**Table 2. Summary of sequential model for Kidney risk classification using GRU Unit layer and dense Units**

| Layer (type) | Output Shape | Parameters |
|---|---|---|
| GRU Unit | 32 | 3360 |
| Droput | 32 | 0 |
| Dense | 1 | 33 |
| Total Parameters | | 3393 |
| Trainable Parameters | | 3393 |
| No - Trainable Parameters | | 0 |

### 3.2.2. RUSP-Net Model for Kidney tumor Segmentation

The proposed RUSP-Net model is an extension of the classic UNet [26] model thatcombines an encoder-decoder architecture with residual connections [31], spatial pyramid
pooling module [32], and dilated convolutions [33]. The architecture of the proposed model .

**Figure 5. CT scan image segmentation using Residual UNet with pyramid and dilated convolutionsfor semantic segmentations with low trainable**

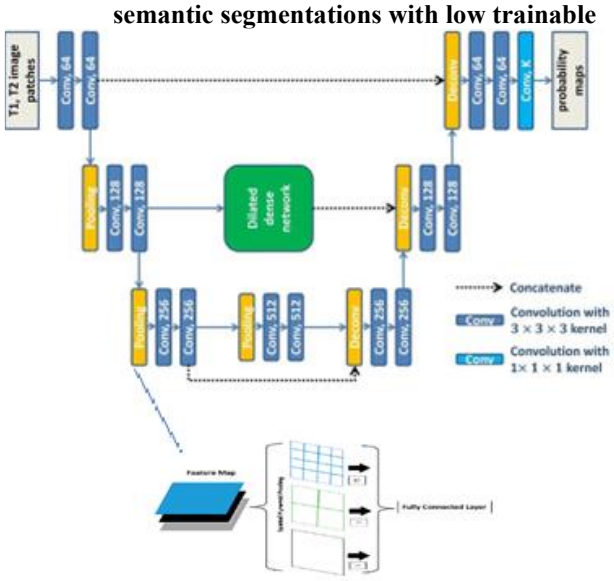


The encoder consists of a series of convolutional blocks that down sample the inputimage. Each block comprises two 3×3 convolutional layers followed by batch normalization 212 and a ReLU activation function, and a 2×2 max-pooling operation. Let X be the input image output of the encoder. 213and Henc(x) be the Then, the output feature maps of the i-th blockof the encoder, Hi(x), are computed described in equation (5). Hi(x) = relu(conv(Hi-1(x)) (5)where conv denotes the 3×3 convolution operation, relu denotes the ReLU [34] activation function, and Hi-1(x) denotes the output feature maps of the (i-1)-th block of the encoder. The decoder consists of a series of convolutional blocks that upsample the feature maps to the original resolution. Each block comprises a 2×2 transposed convolutional layer followed by concatenation with the corresponding feature maps from the encoder and two 3×3 convolutional layers with batch normalization and a ReLU activation function. Let Hdec(x) be the output of the decoder. Then, the output feature maps of the i-th block of the Gi(x) = relu(conv(concat(Gi-1(x),Hi-1(x)))) in equation (6): (6) where concat denotes decoder, Gi(x), arecomputed as shown the concatenation operation, conv denotes the 3×3 convolution operation, relu denotes the ReLU [34] activation function, Gi-1(x) denotes the output feature maps of the (i-1)-th block of the decoder, and Hi-1(x) denotes the corresponding feature maps from the encoder. In addition to the skip connections, the proposed model also includes residual connections between the layers of the encoder and decoder. The residual connections allow for the model to learn more complex features and improve its overall performance. Let Ri(x) be the output of the residual connection between the i-th block of the

encoder and decoder. Then, the residual connections are calculated as shown in equation (7). Ri(x) = Hi(x) + Gi(x) (7) The proposed model also includes the use of a spatial pyramid pooling module, which allows for the model to learn features at multiple scales. The spatial pyramid pooling module is added to the final layer of the encoder, before the feature maps are passed to the decoder. The spatial pyramid pooling module comprises three parallel 3×3 convolutional layers with different dilation rates (1, 2, and 3), followed by concatenation. The output feature maps of the spatial pyramid pooling module are denoted by SPP(x). Finally, the proposed model includes the use of dilated convolutions, which allows for the model to have a larger receptive field without increasing the number of parameters. The dilated convolutions are used in the final layers of the decoder, where the feature maps are upsampled to the original resolution. Let Y be the output of the proposed model. Then, the final output feature maps are computed as shown in equation (8). Y = conv(relu(conv(concat(Ri(x), SPP(x)))) (8) where conv denotes the 3×3 convolution operation, relu denotes the ReLU activation function, concat denotes the concatenation operation, Ri(x) denotes the residual connection between the i-th block of the encoder and decoder, and SPP(x) denotes the output feature maps of the spatial pyramid pooling module. Overall, the proposed model improves upon the classic UNet [26] architecture by adding residual connections, a spatial pyramid pooling module, and dilated convolutions. To reduce the number of parameters in the model, pruning techniques can be applied to the convolutional layers in the contracting and expanding paths. The pruned model will have a smaller number of weights and can be more easily deployed on resource-constrained devices [35]. Overall, a lightweight pruned UNet model with depthwise separable convolution [35] can achieve high accuracy in kidney tumor segmentation while minimizing computation and memory requirements.

### 3.3. Distributed Fusion Segmentation Model

The Distributed deep learning model [36] designed to predict the presence of kidney tumors using both medical imaging data and clinical data. The model is split into two parts: a lightweight pruning depth-wise separable convolution model [35] for the imaging data, and a GRU model [30] for the clinical data. The proposed model is to improve the accuracy of kidney tumor detection by leveraging the complementary information provided by both imaging and clinical data. By training the model in a distributed manner, the computational workload can be divided among multiple nodes, making it possible to process large datasets efficiently. The proposed model Distributed Fusion Segmentation (DFS) shown in Fig 6 training process involves partitioning the data into multiple subsets, assigning each subset to a worker node, and training each node's model replica on its assigned subset using stochastic gradient descent. The gradients computed by each worker node are averaged across all nodes to obtain a global gradient update, which is then used to synchronize the weights of each model replica. The model is trained iteratively until convergence, at which point the predictions of each model replica are aggregated to obtain the final prediction for each input.

**Figure 6. The proposed architecture of Distributed Fusion Segmentation (DFS) for Kidney tumor segmentation and its progression using CT scan image, clinical data records.**

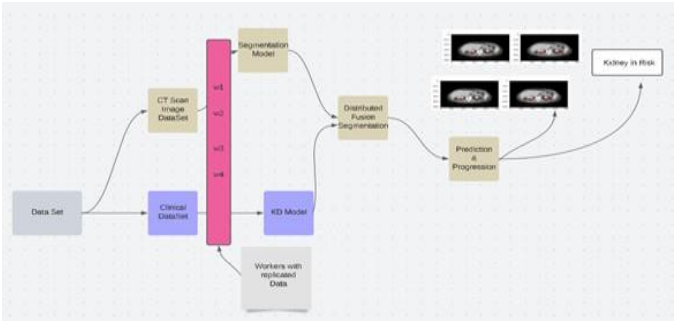


The proposed algorithm shown in Fig 7 involves training separate models for seg- 271 mentation and feature extraction, and then fusing the results using a fusion model. The 272 algorithm uses stochastic gradient descent (SGD) [37] with weight averaging to train the 273 models in a distributed [36] manner. The final segmentation and probability map are ob- 274 tained by aggregating the predictions of each model replica. The postprocessing step is used 275 to improve the accuracy of the segmentation and probability map, and the visualization 276 step is used to aid in clinical decision making

**Figure 7. Distributed Fusion Segmentation Algorithm for CT scan images consist of slices with ground truth segmentation and clinical records to classify kidney risk factors.**

1) Initialize the weights of the models $f(X_{img}; W_{img})$ and $g(X_{clinical}; W_{clinical})$.
2) Partition the data X into P subsets $X_1, X_2, ..., X_P$ and assign each subset to a worker node i.
3) Repeat until convergence or a maximum number of iterations is reached:
   a) On each worker node i, perform the following steps:
      i) Load the CT scan images and clinical data in subset $X_i$.
      ii) Compute the segmentation mask using the model $f(X_{img}; W_{img})$ and the CT scan images (1) in $X_i$.
      iii) Extract features from the clinical data in Xi using the model $g(X_{clinical}; W_{clinical})$.
      iv) Fuse the segmentation mask and clinical features using a fusion model to obtain a probability map.
      v) Compute the loss function L using the ground truth labels and the probability map.
      vi) Compute the gradients with respect to the local weights: $?W_i L$
   b) Average the gradients across all worker nodes to obtain the global gradient update:
      $?W L = (1/P) \Sigma_i ?W_i L$
   c) Synchronize the weights of each model replica using an all-reduce operation:
      $W_i ? W_i - \eta * ?W L$
4) Aggregate the predictions of each model replica to obtain the final segmentation and probability map for each input.
5) Postprocess the final segmentation and probability map to remove false positives and refine the tumor boundaries.
6) Visualize the final segmentation and probability map to aid in clinical decision making.

## Results

This section presents the experiment results of Clinical-GRU model, RUSP-Net CT scan image segmentation and the proposed model Distributed Fusion Segmentation (DFS) model for Kidney Tumor Segmentation and its progression. The model run with often the hyperparameters, though all had different network architectures. Results are discussed in the following current section. The Clinical-GRU classification model effectiveness on the KD dataset is demonstrated through several performance metrics, including the false positive rate (FPR), false negative rate (FNR), sensitivity, specificity, accuracy, F-score, and kappa value. To evaluate the classification performance of any classifier, the confusion matrix is essential. It is a 2x2 matrix that provides information about the actual and predicted classifications. The confusion matrix includes four elements: true positives (TP), true negatives (TN), false positives (FP), and false negatives (FN). These four elements are used to calculate various classification measures for the proposed model. The described measurements are calculated for the clinical data described in Section 3.

**Table 3. Performance of clinical records by applying proposed GRU-deep learning model**

| Performance Measures) | FPR | FNR | Sensitivity | Specificity | Accuracy | F-Score | Kappa |
|---|---|---|---|---|---|---|---|
| GRU Unit Sequential Model | 6.660 | 4.00 | 96.00 | 93.33 | 97.888 | 97.00 | 90.01 |

Table 3 provides the obtained FS results obtained by the proposed deep learning model. Fig 8 shows the gradual increasing of the classifier accuracy from 85.00 to 97.88 with number of epochs.is shown in Fig 5 and it is presented in the current section.

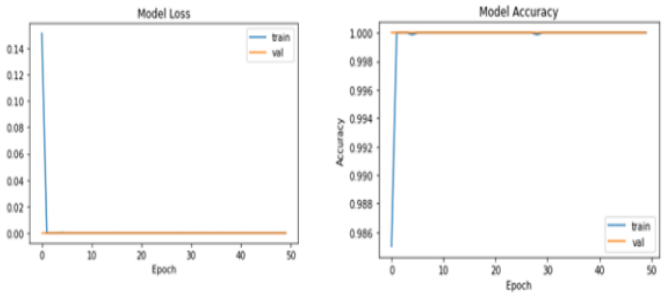


**Figure 8. Model Loss and Accuracy of Kidney Risk classification using proposed sequential deep learning model which is described in Section 3.**

The SHAP[38] is an additive feature attribution method that provides an explanation of the tree ensemble's [39] over impact in the form of particular feature contribution and relatively consistent with human intuition. SHAP [38] plot can give physicians an intuitive understanding of key feature in the model and it visually displays the top risk factors Figure 9. Hemoglobin in gms (hemo) , Serum Creatinine in mgs/dl (sc), Diabetes Mellitus(dm), Hypertension(htn), Sugar(su) were associated with higher risk probability of adverse outcomes in patients with kidney disease.

**Figure 9. High Risk factors of kidney disease for prognosis.**

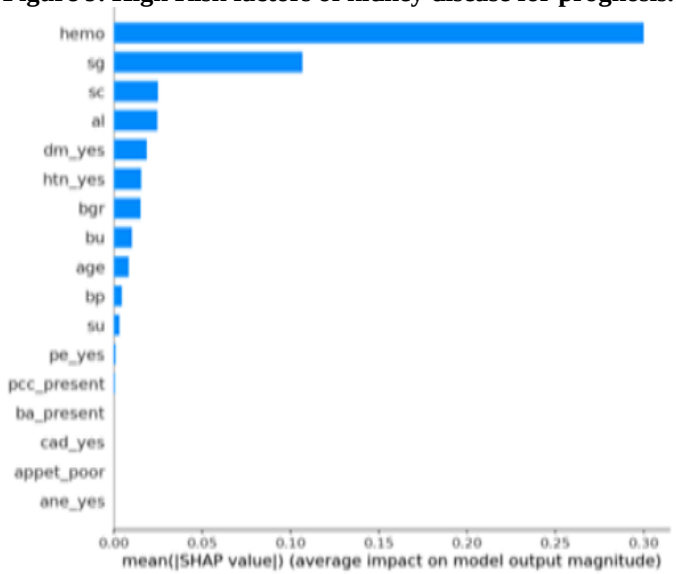


The proposed RUSP-Net network is trained with the kidney and kidney tumor region as outputs. The weight updates performed with Adam optimizer [40] using a learning rate of 0.001 and reduced after ten epochs to 10 percentages if there are no improvements in the validation loss. The batch size is chosen to 16, and the total epochs are set to 100. The training was based on Keras with a Tensor Flow backend as a Google Colab deep learning framework enabled with a NVidia GPU such as T4(15 GB memory) with a high-memory VM.

To evaluate the proposed RUSP-Net model's performance, the standard Dice score is considered an evaluation metric. We were provided with 35865 and 10158 images as a training and validation images for our experimentation. Table 4 shows the segmentation results of the proposed RUSP-Net model for training and validation images. From the table, it is observed that, during training, the proposed method achieves the training accuracy of 0.98 shown in Figure 10 for the tumor region. Similarly, our network computational resource usage is shown in Table 4 and 5. From the experimental results, we understand the power of pruning, skip connections residual units and dilated sparsity pyramid pooling in the proposed network. Since adding network pruning to the proposed architecture and skip connections, the total number of flops and parameters is two times smaller than the typical UNet architecture.

**Table 4. Comparison of results between RUSP Net and other models**

| (Model) | Training Loss | Training Accuracy | Mean IoU |
|---|---|---|---|
| U-Net | 0.5601 | 97.87 | 0.435 |
| U-Net (Depthwise + BN) | 0.4439 | 93.62 | 0.362 |
| RUSP-Net (Proposed Model) | 0.066 | 98.43 | 0.428 |

**Table 5. Calculating the Number of parameters and floating-point operations for the proposed model**

| Model) | Number of Parameters | Number of Flops |
|---|---|---|
| Classical UNet | 31,031,745 | 27352612872.00 |



DOI: 10.5123/inj.2024.1.inj46
ISSN:2093-4777 | E-ISSN:2093-6931
Vol. 28 Iss. 1 (2024)

| | | |
|---|---|---|
| RSUP – Net (Proposed Model) | 28,031,745 | 24095637504.00 |

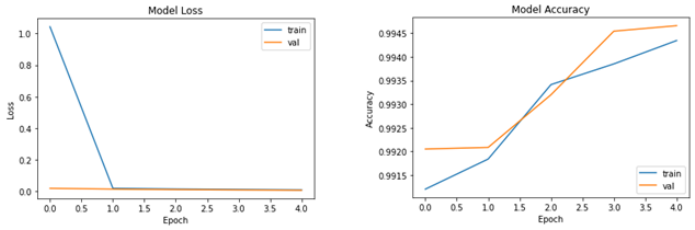


**Figure 10. Kidney tumor segmentation loss and accuracy using CT scan images by applying the proposed model which is described in Section 3**

To evaluate the proposed algorithm Distributed Fusion Segmentation (DFS) we applied on 10000 records with which consists of CT scan images with two classes and clinical features with 2 classes. To apply our proposed DFS the data is partitioned into P subsets to distribute the computation across multiple worker nodes, which will helped to reduce the overall time needed to process the data. In our implementation data is divided into 4 subsets of 2500 records each. Eash subset is balanced by applying overfitting [41] algorithms. The weights of the models are then synchronized across all workers using all reduce operation. Each worker node involved loading the data running the image segmentation and clinical feature extraction models. For the single worker scenario, the entire dataset of 10,000 records would need to be loaded into memory on the single worker node, requiring a total of 65 GB of memory.

**Table 6. Comparison of single worker and four workers Computational inference time for DFS which includes Clinical-GPU and RUSP Net and individual model**

| Iterations | Number of Records Inference Time | Workers |
|---|---|---|
| Clinical- GPU 100 | 10,000 2.18 Hours | Single Worker |
| RUSP-Net 100 | 10,000 13.78 Hours | Single Worker |
| DFS 100 | 10,000 1.74 hours | Four Workers |

The total computation time shown in Table 6, is 10,000 * 0.1 seconds per record * 100 iterations required 27.78 hours. As we applied DFS on 4 workers then total computation inference time is 1.74 hours which shows the fast inference time of our proposed algorithm and results are also descent with 98.001 accuracy Figure 11. And also fusion of tumor segmentation and clinical feature extraction also improves the performance of tumor segmentation and progression.

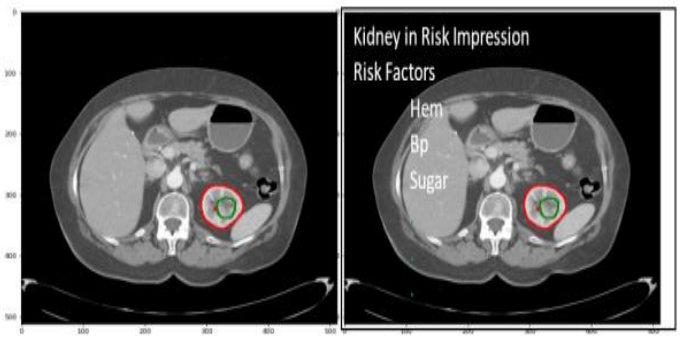


**Figure 11. Result of Distributed Fusion Segmentation ( DFS ) for Kidney tumor Segmentation and Kidney Risk Classification**

## Conclusion and Future Work

In this model, we proposed a Distributed Fusion Segmentation (DFS) approach for 338 kidney tumor

segmentation and clinical data analysis. The model partitions the data and 339 distributes it to worker nodes for training local models using stochastic gradient descent. 340 The models are synchronized using an all-reduce operation to obtain a global gradient 341 update. The final prediction is obtained by aggregating the predictions of each model 342 replica using a weighted averaging scheme. This model has the potential to improve 343 the accuracy and efficiency of kidney tumor segmentation and clinical data analysis, as 344 well as enable the analysis of large-scale healthcare datasets. There are several avenues 345 for future work that can improve the performance and applicability of this distributed 346 machine learning approach for healthcare applications. One potential area of focus is 347 developing more efficient data partitioning strategies that can improve the training time 348 and reduce communication overhead between worker nodes. Additionally, optimizing the 349 hyperparameters of the model, such as learning rate, batch size, and regularization, can 350 further improve the accuracy and efficiency of the model. Another area of future work is 351 investigating the use of transfer learning and model compression techniques to improve 352 the generalization and scalability of the model. Finally, the model can be extended to 353 other healthcare applications, such as disease diagnosis and drug discovery, to improve the 354 overall quality and efficiency of healthcare.

## Funding
No Funding

## Institutional Review Board Statement
Not applicable.

**Informed Consent Statement**
Not applicable.

**Data Availability Statement** To access the KiTs 19 dataset, interested researchers can visit the official website (https://kits19.grand-challenge.org/) The KiTs 19 dataset is a publicly available medical imaging dataset that consists of 300 high-quality CT scans of kidneys.

## Acknowledgments
Princess Nourah bint Abdulrahman University Researchers Supporting Project number (PNURSP2023R432), Princess Nourah bint Abdulrahman University, Riyadh, Saudi Arabia **Conflicts of Interest**
The authors declare no conflict of interest

## References
1. mmirati, A. L. (2020). Chronic kidney disease. In Revista da Associacao Medica Brasileira. https://doi.org/10.1590/1806- 371 9282.66.S1.3 372
2. eiga, M. P. P. da, Arija, I. N., García, L. B., Velarde, L. C., Espinosa, J. C. (2021). Kidney cancer. Medicine (Spain). https://doi.org/10.1016/j.med.2021.02.011 374
3. in, S., Mao, J., Duan, C., Wang, J., Lu, Y., Yang, J., Hu, J., Liu, X., Guan, W., Wang, T., Wang, S., Liu, J., Song, W., Song, X. (2022). Identification and Quantification of Necroptosis Landscape on Therapy and Prognosis in Kidney Renal Clear Cell Carcinoma. Frontiers in Genetics. https://doi.org/10.3389/fgene.2022.832046 377
4. uida, F., Tan, V. Y., Corbin, L. J., Smith-Byrne, K., Alcala, K., Langenberg, C., Stewart, I. D., Butterworth, A. S., Surendran, P., Achaintre, D., Adamski, J., Exezarreta, P. A., Bergmann, M. M., Bull, C. J., Dahm, C. C., Gicquiau, A., Giles, G. G., Gunter, M. J., Haller, T., . . . Johansson, M. (2021). The blood metabolome of incident kidney cancer: A case-control study nested within the MetKid consortium. PLoSMedicine. https://doi.org/10.1371/journal.pmed.1003786 381
5. litcroft, J. G., Verheyen, J., Vemulkar, T., Welbourne, E. N., Rossi, S. H., Welsh, S. J., Cowburn, R. P., Stewart, G. D. (2022). Early detection of kidney cancer using urinary proteins: a truly non-invasive strategy. In BJU International. https://doi.org/10.1111/bju.15601 384
6. celo, G., Larose, T. L. (2018). Epidemiology and risk factors for kidney cancer. In Journal of Clinical Oncology. https://doi.org/10.1200/JCO.2018.79.1905
7. ia, K. jian, Yin, H. sheng, Zhang, Y. dong. (2019). Deep Semantic Segmentation of Kidney and Space-Occupying Lesion Area Based on SCNN and ResNet Models Combined with SIFT-Flow Algorithm. Journal of Medical Systems. https://doi.org/10.1007/s10916- 018-1116-1
8. avikumaran, P., Vimala Devi, K., Valarmathi, K. (2022). An Improved Kidney Tumor Prediction Using Deep Convolutional Neural Network-Restricted Boltzmann Machine Technique in Medical Image Segmentation. Journal of Medical Imaging and Health Informatics.

https://doi.org/10.1166/jmihi.2021.3917 392
9. hongprayoon, C., Hansrivijit, P., Kovvuru, K., Kanduri, S. R., Torres-Ortiz, A., Acharya, P., Gonzalez-Suarez, M. L., Kaewput, W., Bathini, T., Cheungpasitporn, W. (2020). Diagnostics, risk factors, treatment and outcomes of acute kidney injury in a new paradigm. In Journal of Clinical Medicine. https://doi.org/10.3390/jcm9041104
10. iras, D., Masala, M., Delitala, A., Urru, S. A. M., Curreli, N., Balaci, L., Ferreli, L. P., Loi, F., Atzeni, A., Cabiddu, G., Racugno, W., Ventura, L., Zoledziewska, M., Steri, M., Fiorillo, E., Pilia, M. G., Schlessinger, D., Cucca, F., Rule, A. D., Pani, A. (2020). Kidney size in relation to ageing, gender, renal function, birthweight and chronic kidney disease risk factors in a general population. Nephrology Dialysis Transplantation. https://doi.org/10.1093/ndt/gfy270
11. asic, V., Janchevska, A., Emini, N., Sahpazova, E., Gucev, Z., Polenakovic, M. (2016). Chronic kidney disease - pediatric risk factors. In Prilozi (Makedonska akademija na naukite i umetnostite. Oddelenie za medicinski nauki). https://doi.org/10.1515/prilozi- 401 2016-0003
12. ian, S. Z., Hong, W. D., Lingjie-mao, Chenfeng-lin, Zhendong-fang, Pan, J. Y. (2020). Clinical Characteristics and Outcomes of Severe and Critical Patients With 2019 Novel Coronavirus Disease (COVID-19) in Wenzhou: A Retrospective Study. Frontiers in Medicine. https://doi.org/10.3389/fmed.2020.552002 405
13. ergieva, S., Mangaldgiev, R., Dimcheva, M., Nedev, K., Zahariev, Z., Robev, B. (2021). SPECT-CT imaging with [99mTc]PSMA-T4 in patients with recurrent prostate cancer. Nuclear Medicine Review. https://doi.org/10.5603/NMR.2021.0018
14. oni, M. O. F., Matin, A., Hasan, T., Sarker, M. R. I. (2022). Performance Analysis of Classifier for Chronic Kidney Dis- ease Prediction Using SVM, DNN and KNN. In Lecture Notes on Data Engineering and Communications Technologies. https://doi.org/10.1007/978-981-16-6636-0_1 **15.** umar, K., Abhishek, A. (2012). Artificial Neural Networks for Diagnosis of Kidney Stones Disease. International Journal of Information Technology and Computer Science. https://doi.org/10.5815/ijitcs.2012.07.03
15. onnelly, L. (2020). Logistic regression. MEDSURG Nursing. https://doi.org/10.46692/9781847423399.014
16. reiman, L. (2001). Random forests. Machine Learning. https://doi.org/10.1023/A:1010933404324
17. ongbo, O. A., Adetunmbi, A. O., Ogunrinde, R. B., Badeji-Ajisafe, B. (2020). Development of an ensemble approach to chronic kidney disease diagnosis. Scientific African. https://doi.org/10.1016/j.sciaf.2020.e00456
18. oo, K. D., Noh, J., Lee, H., Kim, D. K., Lim, C. S., Kim, Y. H., Lee, J. P., Kim, G., Kim, Y. S. (2017). A Machine Learning Approach Using Survival Statistics to Predict Graft Survival in Kidney Transplant Recipients: A Multicenter Cohort Study. Scientific Reports. https://doi.org/10.1038/s41598-017-08008-8
19. radeep, T., Bardhan, A., Burman, A., Samui, P. (2021). Rock strain prediction using deep neural network and hybrid models of anfis and meta-heuristic optimization algorithms. Infrastructures. https://doi.org/10.3390/infrastructures6090129 **21.** ibley, K. G., Girges, C., Hoque, E., Foltynie, T. (2021). Video-Based Analyses of Parkinson's Disease Severity: A Brief Review. In Journal of Parkinson's Disease. https://doi.org/10.3233/JPD-202402
20. **22**. slam Ayon, S., Milon Islam, M. (2019). Diabetes Prediction: A Deep Learning Approach. International Journal of Information Engineering and Electronic Business. https://doi.org/10.5815/ijieeb.2019.02.03
21. **23**. hafi, T., Matsushita, K., Selvin, E., Sang, Y., Astor, B. C., Inker, L. A., Coresh, J. (2012). Comparing the association of GFR estimated by the CKD-EPI and MDRD study equations and mortality: The third national health and nutrition examination survey (NHANES III). BMC Nephrology. https://doi.org/10.1186/1471-2369-13-42
22. **24**. oulami, K. B., Kaabouch, N., Saidi, M. N., Tamtaoui, A. (2021). Breast cancer: One-stage automated detection, segmentation, and classification of digital mammograms using UNet model based-semantic segmentation. Biomedical Signal Processing and Control. https://doi.org/10.1016/j.bspc.2021.102481
23. **25**. hu, X., Zhou, Y., Li, F., Zhou, T., Meng, X., Wang, F., Zhang, Z., Pu, J., Xu, B. (2021). Three-dimensional semantic seg- mentation of pituitary adenomas based on the deep learning framework-nnU-net: A clinical perspective. Micromachines. https://doi.org/10.3390/mi12121473 434
24. **26**. sensee, F., Petersen, J., Klein, A., Zimmerer, D., Jaeger, P. F., Kohl, S., Wasserthal, J., Koehler, G., Norajitra, T., Wirkert, S., Maier-Hein, K. H. (2019). nnU-Net: Self-adapting Framework for U-Net-Based Medical Image Segmentation. Informatik Aktuell. https://doi.org/10.1007/978-3-658-25326-4_7
25. **27**. sai, Y.-C., Sun, Y.-N. (2019). KiTS19 Challenge Segmentation.

https://doi.org/10.24926/548719.021
26. **28**. .Swathi Baby, T. Panduranga Vital. (2015). Statistical Analysis and Predicting Kidney Diseases using Machine Learning Algorithms. International Journal of Engineering Research And. https://doi.org/10.17577/ijertv4is070234
27. **29**. ang, W. C., Cheng, D. Z., Yao, T., Yi, X., Chen, T., Hong, L., Chi, E. H. (2021). Learning to Embed Categorical Features without Embedding Tables for Recommendation. Proceedings of the ACM SIGKDD International Conference on Knowledge Discovery and Data Mining. https://doi.org/10.1145/3447548.3467304
28. **30**. ajjad, M., Khan, Z. A., Ullah, A., Hussain, T., Ullah, W., Lee, M. Y., Baik, S. W. (2020). A Novel CNN-GRU-Based Hybrid Approach for Short-Term Residential Load Forecasting. IEEE Access. https://doi.org/10.1109/ACCESS.2020.3009537
29. **31**. iang, H., Zhao, X. (2021). Rolling Bearing Fault Diagnosis Based on One-Dimensional Dilated Convolution Network with Residual Connection. IEEE Access. https://doi.org/10.1109/ACCESS.2021.3059761
30. **32**. bdani, S. R., Zulkifley, M. A., Zulkifley, N. H. (2021). Group and shuffle convolutional neural networks with pyramid pooling module for automated pterygium segmentation. Diagnostics. https://doi.org/10.3390/diagnostics11061104
31. **33**. ang, Z., Ji, S. (2021). Smoothed dilated convolutions for improved dense prediction. Data Mining and Knowledge Discovery. https://doi.org/10.1007/s10618-021-00765-5
32. **34**. anerjee, C., Mukherjee, T., Pasiliao, E. (2020). The Multi-phase ReLU Activation Function. ACMSE 2020 - Proceedings of the 2020 ACM Southeast Conference. https://doi.org/10.1145/3374135.3385313
33. **35**. ao, P. K. (n.d.). WP-UNet: Weight Pruning U-Net with Depthwise Separable Convolutions for Semantic Segmentation of Kidney Tumors. 1–19.
34. **36**. anger, M., He, Z., Rahayu, W., Xue, Y. (2020). Distributed Training of Deep Learning Models: A Taxonomic Perspective. In IEEE Transactions on Parallel and Distributed Systems. https://doi.org/10.1109/TPDS.2020.3003307
35. **37**. ottou, L. (2012). Stochastic gradient descent tricks. Lecture Notes in Computer Science (Including Subseries Lecture Notes in Artificial Intelligence and Lecture Notes in Bioinformatics). https://doi.org/10.1007/978-3-642-35289-8_25
36. **38.** eMaere, M. Z., Lauro, F. M., Thomas, T., Yau, S., Cavicchioli, R. (2011). Simple high-throughput annotation pipeline (SHAP). Bioinformatics. https://doi.org/10.1093/bioinformatics/btr411
37. **39**. oore, A., Cai, Y., Jones, K., Murdock, V. (2017). Tree Ensemble Explainability. International Conference on Machine Learning.
38. **40**. onur, O. (2013). Adam Optimizer. In Energy Education Science and Technology Part B: Social and Educational Studies.
39. **41**. rownlee, J. (2016). Overfitting and Underfitting With Machine Learning Algorithms. Machine Learning Mastery